View metadata, citation and similar papers at core.ac.uk
brought to you by CORE
provided by Ghent University Academic Bibliography

Proceedings of 9th International Symposium on Fluid-Structure Interactions, Flow-Sound Interactions, Flow-Induced Vibration & Noise
July 8-11, 2018, Toronto, Ontario, Canada

FIV2018-132

SIMULATIONS OF A FLEXIBLE CYLINDER IN A CONFINED REGION USING A CHIMERA TECHNIQUE

Lucas Delcour*
Ghent University
Belgium
lucas.delcour@ugent.be

Jan Vierendeels
Ghent University, Flanders Make
Belgium
jan.vierendeels@ugent.be

Joris Degroote
Ghent University, Flanders Make
Belgium
joris.degroote@ugent.be

ABSTRACT

Fluid-structure interaction (FSI) simulations involving the motion of flexible structures within confined regions are often hindered by mesh degradation when an arbitrary Lagrangian-Eulerian (ALE) approach is used. In this paper the feasibility of using an overset or Chimera methodology for this kind of simulations is investigated. More specifically, simulations are performed to investigate the motion of a yarn within the main nozzle of an air-jet weaving loom. The overset mesh, surrounding the flexible structure (the yarn), is superimposed on a fixed background mesh, which covers the entire flow domain. The overset mesh is not confined to the physical fluid domain allowing for larger structural deformations without severe grid degradation. To assess the limitations and errors associated to the use of an overset grid fluid-structure interaction simulations are performed with varying degrees of freedom for the structure. The flow is calculated based on the compressible Reynolds-averaged Navier-Stokes equations as both high and low Mach number flows are considered. For high Mach number flows, the nozzle geometry used in the fluid-structure interaction simulations is subjected to shocks. The presence of these shocks should be taken into account when constructing the overset grid.

INTRODUCTION

The study of the motion of flexible cylinders subjected to axial flow has mainly received attention in the light of heat exchangers and nuclear reactors. Païdoussis [1] analysed the behavior of such structures based on the derived equations of motion. Accounting for complex flow structures, such as flow separation, turbulence, vortices and shocks, often requires that one resorts to numerical methods. This was for example done by De Moerloose et al. for vortex induced vibration in an array of tube bundles subjected to axial flow [2]. In the current research the motion of a yarn within the main nozzle of an air-jet weaving loom is studied.

In air-jet weaving looms the main nozzle generates a high-speed air flow which accelerates the yarn up to the insertion speed. Once the yarn leaves the main nozzle it enters the reed channel, where relay nozzles further support the motion. To achieve high production speeds two conditions have to be satisfied. Firstly, the insertion speed has to be sufficiently high. Secondly, the number of miss-insertions has to be limited. The insertion of a yarn with an air-jet weaving loom is, however, not a positively controlled process and its success depends on the interaction between the air flow and the yarn.

To improve the performance of air-jet weaving looms, several attempts have been made to model the dy-

namic behavior of a yarn.

Uno [3] and Adanur and Mohamed [4, 5] established numerical methods to estimate the yarn velocity for a single nozzle air jet insertion based on derived equations of motion and empirical models for the air flow velocity and drag force coefficients. Nosraty et al. [6] later established their own model relying on, among others, the model from Adanur and Mohamed. Using their model they numerically calculated the yarn velocity and acceleration. Contrary to above works, which focussed on single nozzle insertion, Celik and Babaarslan [7] set up a model to calculate the weft velocity in air-jet weaving looms with relay nozzles and a reed, using similar techniques.

Previously cited works considered the yarn as a straight, rigid cylinder and often incorporated yarn unwinding forces using mathematical models. Vangheluwe et al. [8] were amongst the first to represent the yarn as a flexible structure. They used their structural model to study distribution of yarn tension during insertion on projectile and rapier looms. Tang and Advani [9] and Kondora and Asendrych [10] studied the motion of flexible fibres suspended in a fluid. De Meulemeester et al. [11] performed simulations concerning the behavior of a flexible yarn as it is pulled from a drum by a main nozzle.

The latter three works, listed in the previous paragraph, can be categorized as one-way fluid-structure interaction (FSI) simulations since the influence of the structural motion on the flow was neglected. For the motion of the yarn within the main nozzle, the interaction between the structure and the fluid can, however, have a substantial influence. Capturing these effects requires the use of two-way FSI simulations. Pei and Yu [12] performed 2D, two-way FSI simulations of the fiber motion inside the air jet nozzle of a vortex spinning machine. They considered the flow to be incompressible, used a monolithic approach and an arbitrary Lagrangrian-Eulerian (ALE) formulation. Wu et al. [13] also performed 2D, two-way FSI simulations. Their focus was on the yarn whipping at the exit of a main nozzle in an air-jet weaving loom. Osman et al. [14] established a method combining a 3D structural model with a 2D, axisymmetric flow model by incorporating an additional source term into the flow equations. Later, Osman et al. [15] performed 3D, two-way FSI simulations to model the motion of a yarn inside the main nozzle, fixed at the yarn inlet. In this research an ALE approach was employed, but the flow time that could be simulated was limited due to mesh degradation. The current research, to some extent, continues the work of Osman et al. [15]. By using a Chimera technique, the mesh deformation can be simplified and mesh degradation can be diminished. The use of a Chimera technique also shows good promise for incorporation of the axial yarn motion into the simulations. Eventually, this could provide a way of simulating the insertion of a flexible yarn for an air-jet weaving loom.

SIMULATION SETUP

Flow model

As mentioned previously, a Chimera technique will be used in this research. This implies that 2 or more separate meshes are superimposed. For the case under consideration it suffices to use a single background and a single component mesh. The background mesh fills up the complete flow domain, for which a meriodional section of the geometry is depicted in Figure 1. The component mesh contains the yarn and is then superimposed onto the background grid. Figure 2 displays the associated geometry. Both meshes are comprised of hexahedral cells; the background and component mesh respectively contain about 1 million and 300 000 cells.

The transient flow field is calculated based on the Reynolds-averaged Navier-Stokes equations (RANS) using an Arbitrary-Lagrangian Eulerian formulation on the component mesh to incorporate the yarn motion. The mesh deformation is restricted to the component mesh; the background mesh remains stationary. As turbulence model the k-ω SST model is selected. A pressure-based solver with the coupled pressure-velocity scheme is used. For compatibility reasons a first-order implicit time discretisation had to be employed. For the convective terms in the density, momentum and energy equations a second-order upwind scheme is used. All flow simulations have been performed using Fluent 18.1 (Ansys, Inc.).

Structural model

The structural model consists of the yarn, represented as a cylinder and an analytical rigid body for contact detection between the yarn and the acceleration tube. The yarn mesh consist of 4800 elements. A visual representation can be found in Figure 3.

Two different cases are considered. In one case the yarn is considered to be flexible and fixed at the left end. In the other case all elements from the structural body are

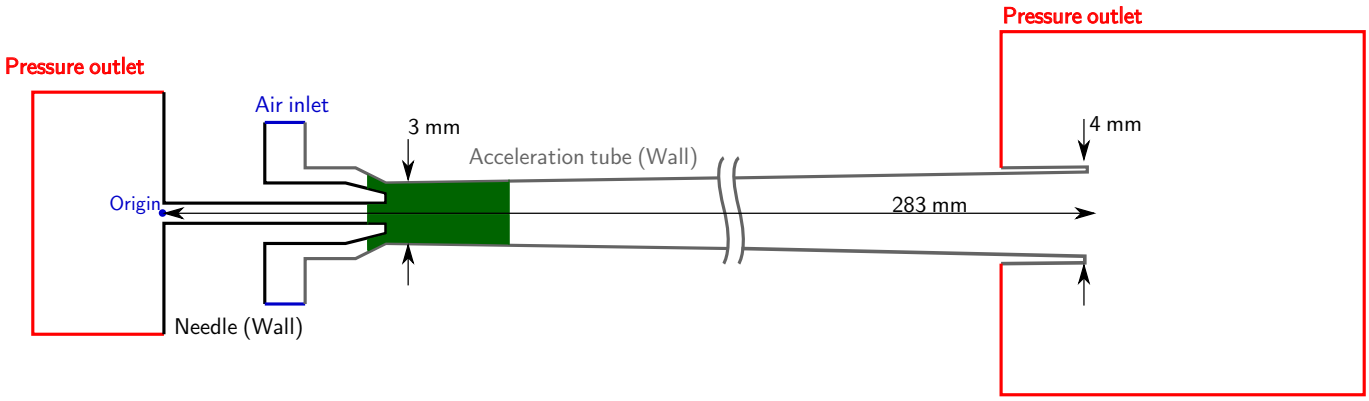

FIGURE 1: Sketch of the flow domain, the main nozzle is severely enlarged in the vertical direction for clarity purposes. The green zone indicates the mixing region.

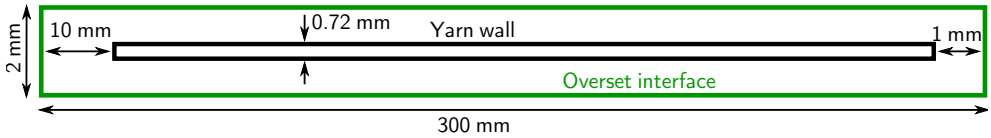

FIGURE 2: Sketch of the geometry for the component mesh.

associated to one rigid body structure. The rigid body is then restricted to motion along the axis of the main nozzle.

The linear density of the yarn is set 464 tex, its Young's modulus to 250 GPa and the Poisson ratio to 0.39. The analytical rigid body has 15% smaller radial dimensions than the actual tube. This is done so that in the flow solver there can always be some cells in between the yarn and the tube wall. The pressure and viscous forces obtained from the flow solver are imposed on the cylinder surfaces and gravity is enabled. The contact between the yarn and the wall is modeled as a frictionless contact. The structural equations are solved using a Hilbert-Hughes-Taylor implicit time discretisation. Structural simulations have been performed in Abaqus 6.14 (Simulia).

Coupling

The coupling between both solvers is achieved using the in-house code "Tango". The interface Quasi-Newton technique with an approximation of the inverse of the Jacobian from a least-squares model (IQN-ILS) has been used (Degroote et al. [16]).

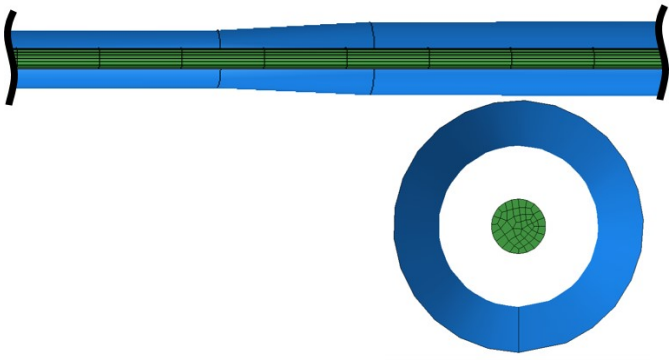

FIGURE 3: Visual representation of the structural model.

RESULTS

Rigid Axial Motion

In these first simulations, the yarn is treated as a rigid body. Only motion along the nozzle axis is allowed for. At the air inlet a pressure profile is imposed, which has been measured experimentally during a yarn insertion. The physical relevance of the simulations is limited to the point at which the yarn's left end passes the jet inlet of the main nozzle. The goal of these simulations was to verify the feasibility of incorporating axial motion with the Chimera methodology. The duration of the simulations

could be extended by accommodating more yarn into the flow domain. This, however, requires that both the flow domain and the structural model are extended axially, increasing the computational cost per time step. In Figure 4 the motion of the yarn is illustrated. Figure 5 depicts the calculated yarn velocity and the applied pressure profile. Figure 6 provides a zoomed in view of the obtained velocity field.

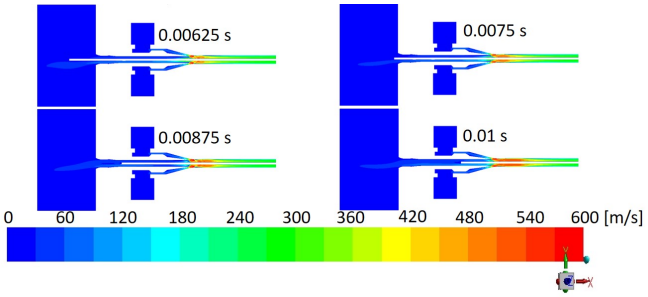

FIGURE 4: Illustration of the rigid axial yarn motion.

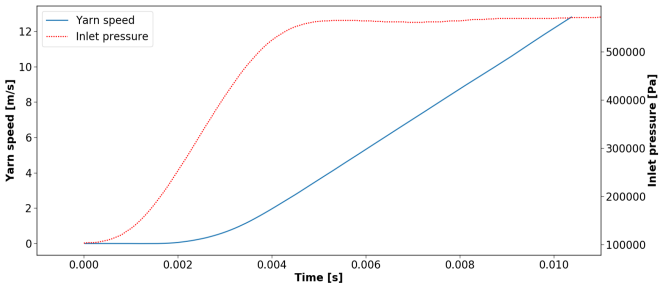

FIGURE 5: Yarn velocity and inlet pressure in function of time.

In Figure 6 it can be seen that the axial resolution of the component mesh (visible close to the yarn) and the background mesh are quite different, smearing out the solution close to the yarn. This is because a fine axial resolution is required to resolve the shocks in that region.

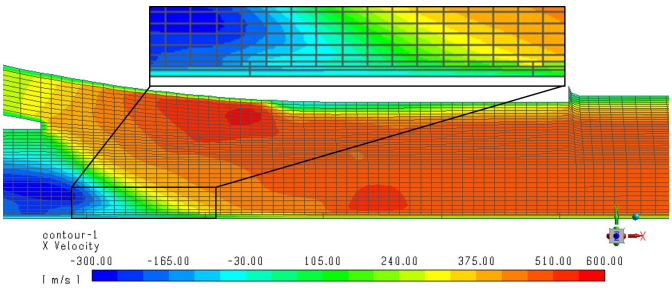

FIGURE 6: Axial velocity magnitude at t = 0.01s in the mixing region (indicated in Figure 1 in green).

Since axial motion of the yarn is involved, it is desirable to have a uniform axial resolution along the yarn. However, applying a fine axial resolution over the entire yarn would entail a large increase in computational cost. If one is only interested in the axial forces on the yarn this poses no real problem. Nevertheless, once the yarn is considered to be flexible, normal forces become important for the yarn deformation and the axial resolution should be treated more carefully. Future simulations will comprise a larger axial domain, allowing for the presence of more yarn and, therefore, a longer simulation time. An experimental procedure could also be established for validation.

Fixed at left end

Simulations have also been performed with the yarn flexible but fixed at the yarn inlet, which is located at x = 0.0 m. These simulations are a continuation of the simulations performed by Osman et al. [15]. Osman et al. used a single three-dimensional fluid grid, which was deformed according to the motion of the yarn. Allthough smoothing techniques were employed, the large yarn deformations eventually degraded the fluid mesh to such an extent that the simulations crashed. By using the Chimera technique a cylindrical mesh can be constructed around the yarn. The yarn displacement only deforms this cylindrical mesh and not the background mesh. The main difference with the use of a single grid is that the component mesh can simply move along with the yarn as it is not constrained by the yarn tube. This allows for large deformations without severe mesh degradation. As the yarn is fixed at the left end, no large axial displacement of the yarn is possible and the axial mesh resolution can easily be matched to that of the background grid. Figure 7 shows some axial cross sections of the component mesh in deformed state. The red lines show the tube position, while the light-gray cylinder represents the yarn. As with the rigid body simulations, a pressure profile is applied to the air inlet but delayed with 4 ms compared to Figure 5.

Figure 8 shows the calculated position of the yarn centerline at several time instants. Do note that the aspect ratio is not respected in the figure (y-displacements appear much larger than they actually are).

Several observations can be made from Figure 8. The curve at 5 ms shows that initially the yarn drops due to gravity, moving it away from the centerline position. From 5.5 ms to 6.35 ms a sudden increase of the deformation occurs at an axial position of about 0.036 m. This

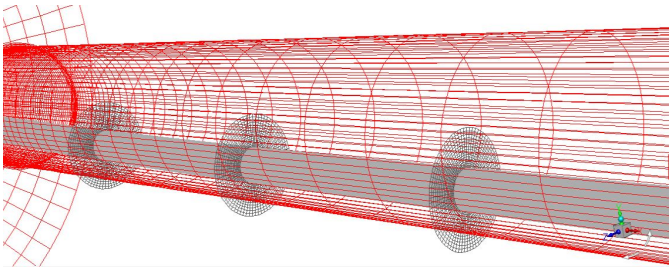

FIGURE 7: Axial cross sections of the component mesh in deformed state at t = 0.0076s.

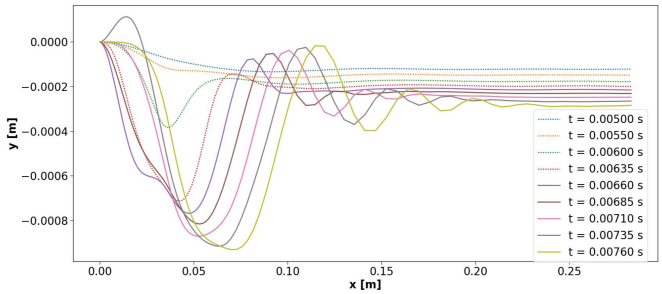

FIGURE 8: Position of the yarn centerline at several time instants. The pressure profile applied at the inlet is the same as in Figure 5 but delayed by 4 ms.

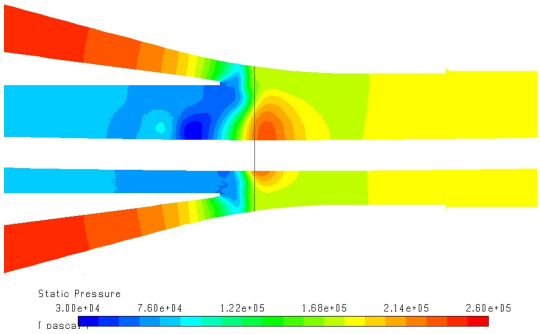

FIGURE 9: Contour plot of static pressure at t = 0.006 s. The black line indicates the position at which x = 0.036 m.

position corresponds to a location slightly behind the jet entrance. The deviation of the yarn from the centerline, due to gravity, causes an asymmetry in the flow. When the pressure starts building up the yarn gets subjected to a pressure gradient pushing it further away from the centerline. This can clearly be seen in Figure 9, which displays a contour plot of the static pressure at t = 6 ms.

In Figure 8 it can also be seen that the yarn takes on a rather distinct shape when moving to t = 6.6 ms. This can

FIGURE 10: Illustration of the contact between the yarn and the analytical rigid body at t = 6.5 ms. The dot is located at an axial coordinate of 0.036 m.

be linked to contact between the yarn and the analytical rigid body. Figure 10 shows the yarn at t = 6.5 ms alongside the analytical body, the dot is located at x = 0.036 m.

Figure 8 also clearly shows a running wave from which a preliminary wavespeed can be extracted. The calculated wavespeeds as listed in Table 1 are obtained by tracking the first peak of the visualized wave. The calculated wavespeeds are of the same order of magnitude as those reported by Osman et al. [15] (typically 30 - 40 m/s). Better comparison and experimental validation, however, require that the simulations are progressed further in time. Currently, the simulated time amounts to 7.67 ms. At regular intervals the minimum orthogonal quality of the mesh was checked and no decrease in mesh quality has yet been observed. As the deformations are already quite large and pressure has nearly reached its peak value it is expected that the simulations can be continued.

TABLE 1: Wavespeeds extracted from Figure 8.

Time [ms]	Axial position [m]	Wavespeed [m/s]
6.60	0.0816	n.a.
6.85	0.0925	43.2
7.10	0.1007	33.0
7.35	0.1098	36.4
7.60	0.1196	39.2

CONCLUSION

In this research a Chimera methodology was employed to simulate the motion of a yarn in the main nozzle of an air-jet weaving loom. This methodology was selected to facilitate the treatment of the dynamic mesh and avoid severe mesh degradation caused by large yarn deformations. Two separate cases were considered. In a first case the yarn was treated as a rigid cylinder, restricted

to axial motion along the centerline of the main nozzle. It was demonstrated that the Chimera methodology can cope with the axial motion despite large differences in axial resolution between the background and component mesh. However, once the yarn is treated as a flexible body it can become important to have a sufficiently fine axial resolution for both meshes. In a second case yarn deformation was allowed and the yarn was fixed at the yarn entrance. Simulations incorporated gravity and contact detection with the tube. The wavespeeds extracted from the simulation correspond reasonably well to those reported by Osman et al. [15], but better comparison requires that the simulations are progressed further in time. Overall no signs of mesh degradation were observed, giving good hope for the continuation of the simulations.

ACKNOWLEDGEMENTS

This work was financially sponsored by a grant from the Special Research Fund of Ghent University. The computational resources (Stevin Supercomputer Infrastructure) and services used in this work were provided by the VSC (Flemish Supercomputer Center), funded by Ghent University, FWO and the Flemish Government department EWI.

REFERENCES

[1] Païdoussis, M. P., 2004. *Fluid-structure interactions: Slender Structures and Axial Flow*, Vol. 2. Elsevier Academic Press London.

[2] De Moerloose, L., Aerts, P., De Ridder, J., Vierendeels, J., Degroote, J., 2018. "Numerical investigation of large-scale vortices in an array of cylinders in axial flow". *Journal of Fluids and Structures,* ***78***, pp. 277–298.

[3] Uno, M., 1972. "A study on air-jet loom with substreams added, part 1: deriving the equation for weft". *Journal of the Textile Machinery Society of Japan,* ***25***, pp. 48–56.

[4] Adanur, S., Mohamed, M. H., 1991. "Analysis of yarn tension in air-jet filling insertion". *Textile Research Journal,* ***61***, pp. 259–266.

[5] Adanur, S., Mohamed, M. H., 1992. "Analysis of yarn motion in single nozzle air-jet filling insertion, part I: Theoretical models for yarn motion". *The Journal of the Textile Institute,* ***81***, pp. 45–55.

[6] Nosraty, H., Jeddi, A. A. A., Mousaloo, Y., 2008. "Simulation analysis of weft yarn motion in single nozzle air-jet loom to study the effective parameters". *Indian Journal of Fibre & Textile Research,* ***33***, pp. 45–51.

[7] Celik, B., Babaarslan, O., 2010. "A Mathematical Model for Numerical Simulation of Weft Insertion on an Air-Jet Weaving Machine". *Textile Research Journal,* ***74***, pp. 236–240.

[8] Vangheluwe, L., Sleeckx, B. Kiekens, P., 1994. "Numerical Simulation Model for Optimisation of Weft Insertion on Projectile and Rapier Looms". *Mechatronics,* ***5***, pp. 183–195.

[9] Tang, W., Advani, S. G., 2005. "Dynamic Simulation of Long Flexible fibers in Shear Flow". *CMES,* ***8***, pp. 165–176.

[10] Kondora, G., Asendrych, D., 2013. "Modelling the Dynamics of Flexible and Rigid Fibres". *Chemical and Process Engineering,* ***34***, pp. 87–100.

[11] De Meulemeester, S., Puissant, P., Van Langenhove, L., 2009. "Three-dimensional Simulation of the dynamic Behavior on Air-jet Looms". *Textile Research Journal,* ***79***, pp. 1706-1714.

[12] Pei, Z., Yu, C., 2010. "Numerical study on the effect of nozzle pressure and yarn delivery speed on the fiber motion in the nozzle of Murata vortex spinning". *Journal of Fluids and Structures,* ***27***, pp. 121–133.

[13] Wu, Z., Chen, S., Liu, Y., Hu, X., 2016. "Airflow characteristics and yarn whipping during startup stage of air-jet weft insertion". *Textile Research Journal,* ***86***, pp. 1988-1999.

[14] Osman, A., Malengier, B., De Meulemeester, S., Peeters, J., Vierendeels, J., Degroote, J., 2017. "Simulation of air-flow-yarn interaction inside the main nozzle of an air jet loom". *Textile Research Journal*, doi: 10.1177/0040517517697646, 11 pages.

[15] Osman, A., Delcour, L., Hertens, I., Vierendeels, J., Degroote, J., 2018. "Toward three-dimensional modeling of the interaction between the air flow and a clamped-free yarn inside the main nozzle of an air jet loom". *Textile Research Journal*, doi: 10.1177/0040517518758006, 12 pages.

[16] Degroote, J., Bathe, K-J, Vierendeels, J., 2009. "Performance of a new partioned procedure versus a monolithic procedure in fluid-structure interaction". *Computers & Structures,* ***87***, pp. 793-801.